Machine learning-based orthotropic stiffness identification using guided wavefield data

Adil Han Orta[a,b,*], Jasper De Boer[c], Mathias Kersemans[b], Celine Vens[c,d], Koen Van Den Abeele[a]

[a] *Wave Propagation and Signal Processing (WPSP), Department of Physics, KU Leuven – Campus Kulak, 8500 Kortrijk, Belgium*
[b] *Mechanics of Materials and Structures (MMS), Department of Materials, Textiles and Chemical Engineering, Ghent University, Technologiepark 46, 9052*
[c] *Department of Public Health and Primary Care, KU Leuven – Campus Kulak, 8500 Kortrijk, Belgium*
[d] *Itec, imec research group at KU Leuven, KU Leuven – Campus Kulak, 8500 Kortrijk, Belgium*

Abstract

The characterization of the full set of elastic parameters for an orthotropic material is a complex non-linear inversion problem that requires sophisticated optimization algorithms and forward models with thousands of iterations. The intricacy of this type of inversion procedure limits the possibility of using these algorithms for large-scale automation and real-time structural health monitoring. At this point, the introduction of machine learning-based inversion strategies might become helpful to overcome the existing limitations of conventional inversion algorithms. In the present study, a multilayer perceptron algorithm is used to identify elastic stiffness parameters of orthotropic

*Corresponding author. Tel: +3293310462
Email addresses: adil.orta@ugent.be (Adil Han Orta), jasper.deboer@kuleuven.be (Jasper De Boer), mathias.kersemans@ugent.be (Mathias Kersemans), celine.vens@kuleuven.be (Celine Vens), koen.vandenabeele@kuleuven.be (Koen Van Den Abeele)

plates using guided wavefield data. A large and diverse training dataset is created by using a semi-analytical finite element model, and the effect of both the training dataset size and the signal-to-noise ratio on the inference outcome are examined. The performance of the multilayer perceptron-based inversion method is first validated on a numerical dataset, and the method is then further applied on experimental data obtained from a multilayered glass-fiber reinforced polyamide 6 composite plate. Finally, the multilayer perceptron-based inference results are compared with the outcome of a traditional inversion algorithm, showing a difference of less than 0.5%.
Keywords: Non-destructive testing, Material characterization, Lamb waves, semi-analytical finite element (SAFE), multilayer perceptron, Orthotropy

1. Introduction

An accurate characterization of material properties is crucial to properly detect, localize, and/or assess damage features in non-destructive testing and structural health monitoring [1]. In literature, researchers have already proposed an extensive set of diagnostic characterization techniques in the last few decades by using natural frequencies [2, 3, 4, 5], bulk wave phase velocities [6, 7], Lamb wave group velocities [8], and Lamb wave dispersion curves [9, 10]. However, these traditional methods employ complex heuristic optimization algorithms, which require thousands of iterations of a forward model to properly identify the stiffness parameters that lead to the best match of the experimental data. These algorithms generally minimize the difference between the measured and the simulated frequency (or time) domain response by adjusting the stiffness parameters using a global heuristic

optimization (genetic algorithm, particle swarm, simulated annealing, etc.). The number of stiffness parameters that can be obtained strongly depends on both the material properties, such as plate thickness and stacking orientation, and the measurement parameters, like the frequency, propagation direction and mode shapes [10]. Moreover, the inversion procedure needs to be repeated for each newly tested material. Therefore, adopting any of these methods for large-scale automation in industry and real-time structural health monitoring is unfeasible.

In recent years, the interest in machine learning and inductive inference has grown exponentially, with applications in a wide range of scientific research areas, covering physics, geology, genetics, medicine, language, etc. In particular, in the field of material characterization, guided ultrasonic waves have been coupled with an uncertainty analysis based on fuzzy arithmetic to identify the material constants of quasi-isotropic fiber-reinforced composites [11]. Bobylev et. al. examined transfer learning algorithms to accurately assess the dynamic behavior of rotor systems with quasi-real-time measurements by estimating single stiffness parameters [12]. Liu et. al. studied the fatigue behavior of wind turbine blades by means of deep learning models using time series stiffness data and estimated the degradation of the structure by assessing a single stiffness parameter with high accuracy [13]. Wei et. al. created a model for isotropic material characterization with an accuracy of about 90% and milliseconds processing time per sample by using convolutional neural network and transfer learning [14]. Obviously, the identification of stiffness parameters for lower material symmetry groups such as transversely isotropic, orthotopic, or monoclinic materials requires more so-

phisticated models. One of the first studies in this field has been performed by Rautela et. al. who explored the possibility of using 1D-convolutional neural networks (CNNs) and recurrent neural networks (RNNs) to identify the elastic properties of transversely isotropic materials [15]. The developed supervised learning algorithms used information on guided wave modes as inputs and considered the elastic properties of the medium as targets. In that particular investigation, the spectral finite element method was implemented as a forward model to create the training data, and relatively large boundaries were used both for the material's density and stiffness parameters to obtain a dataset, consisting of more than 10^4 combinations of different lamina properties. One of the most important conclusions of this study is that the uniqueness of the solution strongly depends on the number of Lamb wave modes that can be discerned in the considered frequency range. In a later study, the effect of noise on the quality of the inversion has been examined by the authors as well [16]. Their results show that a low signal-to-noise ratio significantly increases the error rates for the 1D-CNN, whereas more advanced long short-term memory (LSTM) networks show a better performance for high noise conditions. On the downside, the required computational time per epoch for LSTM networks is almost 30 times higher compared to a 1D-CNN [16].

In another recent study [17], a dual-branch version of CNN was implemented to identify the stacking orientation along with the elastic parameters of transversely isotropic composites using a polar group velocity representation of the A_0 and S_0 modes, calculated via the stiffness matrix method, as input. The study showed that a CNN approach could successfully invert the

material stiffness properties of transversely isotropic composites. In addition, error rates of different machine learning algorithms and their performance, such as support vector machines, random forests, artificial neural networks, etc. have been compared.

Even though classical CNNs have proven to be powerful classification methods for images, video and audio, there are certain limitations. The major limitation can be readily explained by revisiting the example of the polar group velocity images. Whereas the polar group velocity images are used to extract the features to train the network, the polar group velocities themselves strongly depend on the stacking orientation and the in-plane measurement angle. A misalignment of the material, or an unknown material orientation, might lead to polar images with important deviation angles [7]. To account for this, the CNN needs to be learned with a training dataset that includes rotated images. However, this procedure increases the size of the training data which significantly increases the required computational time and power. Alternatively, group equivariant convolutional networks have been proposed and found to perform successfully for a larger group of symmetries, including rotations [18]. A second limitation is that forward models fundamentally calculate discrete wavenumbers, phase, or group velocities. During the conversion of these parameters to images, errors can be introduced as the exact values need to be interpolated to fit the image pixel sizes when the wavenumbers are calculated as solutions of the eigenvalue problem. To circumvent this, a set of forced steady-state equations can be solved directly. However, problems regarding the size of the training data and the need to include rotated images in the training dataset will significantly

increase the required computational time and power.

In the present study, an alternative approach is implemented by using a multilayer perceptron (MLP) method. In the proposed procedure, the semi-analytical finite element (SAFE) model is selected as the forward model to calculate complex wavenumber dispersion curves, due to its accuracy and robustness. Assuming the density and layer orientation for the material to be fixed, the real wavenumbers in different in-plane propagation directions and for a range of frequencies are calculated, and used to create massive training and test datasets for different material property combinations. As such, the MLP approach allows to identify all 9 homogenized elastic stiffness parameters for various materials. The accuracy of this approach is examined with respect to the training dataset size and the noise level. The numerical datasets as well as the code created in Python programming language on Jupyter notebook, used to validate the approach, can be freely downloaded from [19].

The paper is structured as follows. First, in Section 2, the most important aspects of the forward model (SAFE), the experimental wavefield acquisition, and the machine learning model are summarized. Next, Section 3 covers the results of a numerical and an experimental inversion study. Finally, conclusions are given in Section 4.

2. Stiffness Identification Procedure

2.1. Forward model: SAFE

To efficiently calculate the dispersive behavior of Lamb waves for use in the training datasets of the MLP procedure, the approximate method called

the semi-analytical finite element method (SAFE) is adopted in this study [20]. This forward model is implemented, along with a selection of other prediction models, in a standalone MATLAB toolbox called 'The Dispersion Box', which can be downloaded freely from GitHub [21]. The accuracy, as well as the computational efficiency of this method, is extensively discussed in literature [22].

In short, the SAFE method is based on the fact that the homogeneous wave equation in a plate-like medium with orthotropic symmetry can be rewritten as [20]:

$$u^{(e)}(x,y,z,t) = \begin{bmatrix} \sum_{j=1}^{n} N_j(y,z)U_{xj} \\ \sum_{j=1}^{n} N_j(y,z)U_{yj} \\ \sum_{j=1}^{n} N_j(y,z)U_{zj} \end{bmatrix} e^{i(kx-\omega t)} = N(y,z)q^{(e)}e^{i(kx-\omega t)} \qquad (1)$$

where $u^{(e)}(x,y,z,t)$ displacements per element (e), which are expressed in terms of shape functions, $N_j(y,z)$, and the unknown nodal displacement components, $(U_{xj},\ U_{yj},\ U_{zj})$. Further, k is the complex wavenumber, ω is the angular frequency, and n is the number of nodes per element. By using Eq. (1), the strain components ε can be represented as function of the nodal displacements:

$$\varepsilon = \Big[L_x\frac{\partial}{\partial x} + L_y\frac{\partial}{\partial y} + L_z\frac{\partial}{\partial z}\Big]N(y,z)q^{(e)}e^{i(kx-\omega t)} = (B_1 + ikB_2)q^{(e)}e^{i(kx-\omega t)} \quad (2)$$

where $q^{(e)}$ is the unknown nodal displacement for each element, $B_1 = L_yN_{,y} + L_zN_{,z}$, $B_2 = L_xN$. $N_{,y}$ and $N_{,z}$ are the derivatives of the shape function matrix with respect to the y and z directions, respectively. The term L expresses the strain parameters in matrix form, for which the full details can

be found in literature [20]. Finally, the stiffness ($k_1^{(e)}, k_2^{(e)}$ and $k_3^{(e)}$) and mass ($m^{(e)}$) matrices for each element can be calculated as follows:

$$k_1^{(e)} = \int_{\Omega_e} [B_1^T \tilde{C}_e B_1] d\Omega_e, \qquad k_2^{(e)} = \int_{\Omega_e} [B_1^T \tilde{C}_e B_2 - B_2^T \tilde{C}_e B_1] d\Omega_e$$
$$k_3^{(e)} = \int_{\Omega_e} [B_2^T \tilde{C}_e B_2] d\Omega_e, \qquad m^{(e)} = \int_{\Omega_e} [N^T \rho_e N] d\Omega_e, \tag{3}$$

where ρ_e is the density for each element $\tilde{C}_e$ is the complex valued stiffness matrix ($C = C' + jC''$) which is represented as a combination of the elastic (C') and the viscous (C'') parameters. To model the dynamic through-thickness behavior of the entire medium, the mass and stiffness matrices for each element need to be assembled in four global matrices which read as follows:

$$K_1 = \bigcup_{e=1}^{n_{el}} k_1^{(e)}, \qquad K_2 = \bigcup_{e=1}^{n_{el}} k_2^{(e)}, \qquad K_3 = \bigcup_{e=1}^{n_{el}} k_3^{(e)}, \qquad M = \bigcup_{e=1}^{n_{el}} m^{(e)} \tag{4}$$

where n_{el} is the total number of cross-sectional elements. Using the global matrices and imposing energy equilibrium, the homogeneous wave equation can be rewritten as:

$$[K_1 + ikK_2 + k^2 K_3 - \omega^2 M]_M U = 0 \tag{5}$$

The solution of the generalized eigenvalue problem in Eq. 5 yields the (homogenized) complex wavenumber values, $k = k_r + jk_i$, which are characteristic for the plate material (visco-elasticity) and geometry (thickness and stacking). More precisely, the dispersive variation of the real wavenumber (k_r) values with respect to 'frequency $\times$ thickness' (fd) in a fixed in-plane orientation provides the dispersion curves which fundamentally relate to the elastic part of the stiffness tensor (see for example Fig. 1(a) for the case of a 5 mm thick beech wood plate, 0° in-plane direction). On the other hand,

by solving the equation for a fixed fd value for different in-plane propagation directions (ϕ), polar dispersion curves can be obtained, see Fig. 1(b).

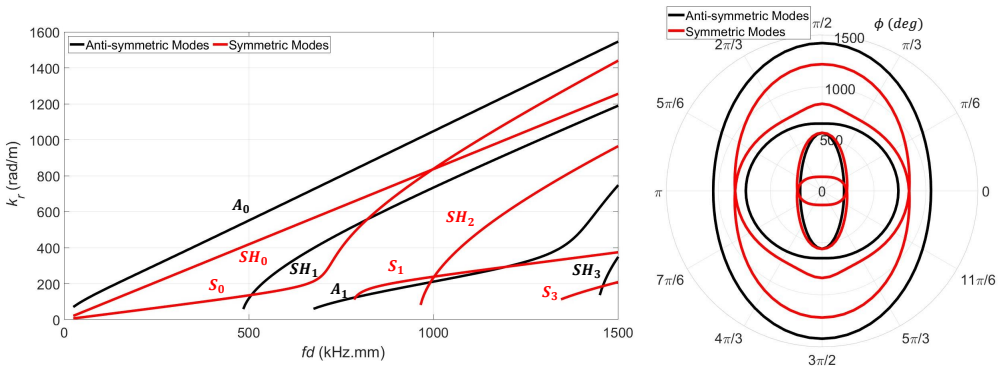

(a) (b)

Figure 1: Wavenumber curves for Lamb waves computed in a vacuumed environment for a 5 mm thick beech wood plate (a) Real Wavenumbers in the frequency range of 10-300 kHz along the $\phi = 0$ direction, and (b) The polar dispersion velocity curve for a fixed frequency $f = 200$ kHz.

2.2. Experimental measurement and Post Processing

For the experimental validation of the ML based inversion method, discussed later in section 3.2, an actual wavefield measurement on a 600 $\times$ 600 $\times$ 5.5 mm Glass Polyamide 6 (G/PA6) UD laminate with stacking sequence $[0/90]_{5s}$ was conducted to test the performance of the proposed MLP method. The plate is excited by a single piezoelectric actuator (type EPZ -20MS64W) positioned at the center of the plate and driven by a voltage amplifier (Falco Systems, type WMA-300). A 16 ms long broadband chirp voltage signal with frequencies between 5 kHz to 300 kHz is used as an excitation signal. The full-field 3D vibrational surface response is recorded by means of an

infrared 3D SLDV (Polytec PSV-500-3D-Xtra) operating on a star-like grid to measure the responses along different in-plane directions, here chosen to cover one quadrant with a measurement at 0, 45 and 90° (See Fig. 2). The three laser heads are set up in an angled configuration to measure both the out-of-plane and in-plane vibrational response with high sensitivity. The sampling rate used to record the vibrational response is 625 kS/s, and the grid step along an in-plane direction is fixed at $D_r \approx 1$ mm. An average over 20 measurements is performed for each point to improve the signal-to-noise ratio. Moreover, the measurement quality is additionally improved by covering the entire surface of the plate with retro-reflective tape. The total amount of time to execute the various experimental line scans along three in-plane directions per sample is about 1 hour. It might be possible to further reduce the measurement time in the future by implementing recent developments in compressed sensing (spatially under sampled measurements), in super-resolution reconstruction using deep learning and in multi-point LDV using on-chip photonics technology [35, 37]. For instance, by using the latter technology, it is possible to measure several points simultaneously, which will reduce the required measurement time significantly. More details about the measurement procedure can be found in literature [10].

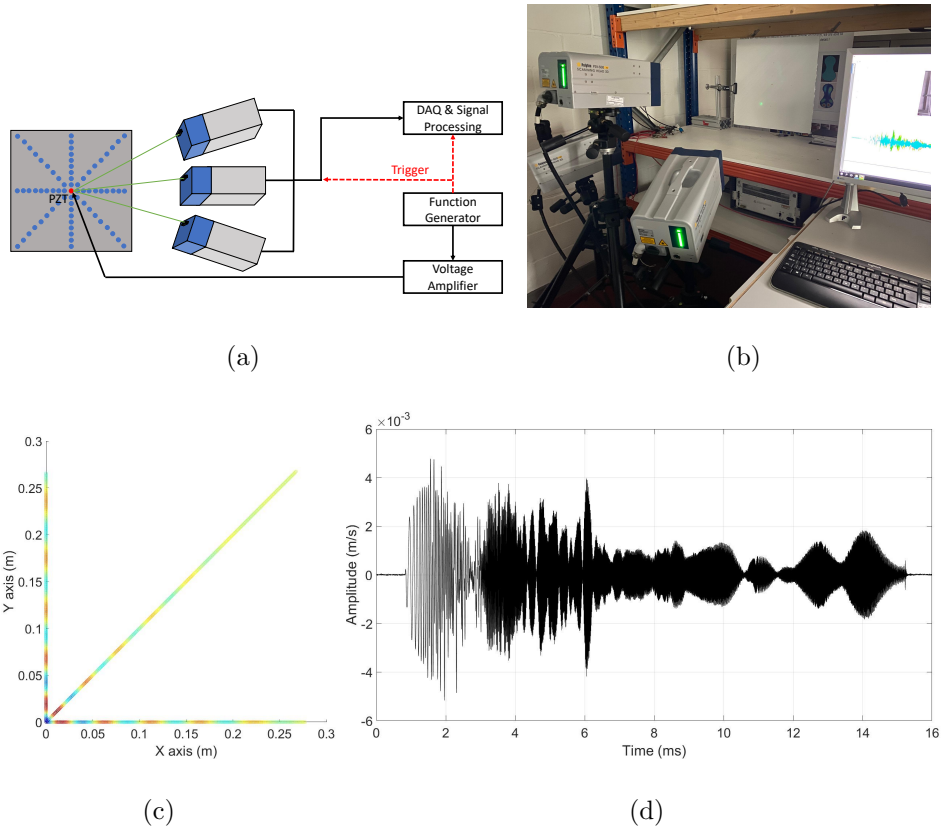

Figure 2: a) Schematic of the experimental procedure, b) Experimental setup, c) The recorded wave propagation on a UD G/PA6 layered plate at t =1.2 ms along a discrete set of angles, and d) The out-of-plane response to a broadband sweep excitation (50-300 kHz in 16 ms) recorded on a 5.5 mm thick UD G/PA6 plate when ϕ=45 at a distance of 15 cm from the actuator.

In terms of post-processing analysis, the measured data in the space-time domain is first converted to wavenumber-frequency domain using a 2D fast Fourier transform. Then, the real wavenumbers are extracted from the magnitude of the wavenumber-frequency map by means of the matrix pen-

cil decomposition method (MPDM). The details as well as the advantages of this extraction procedure for material characterization have already been presented earlier in literature [10]. The implementation of MPDM as part of the post-processing step allows to automatically extract the real wavenumbers (k_r), which comprise the necessary information to identify elastic stiffness parameters. Alternatively, it would also be possible to identify the real wavenumber values manually from the dispersion curves. However, this might lead to relatively high errors and has the drawback that it excludes the use of this characterization method for real-time applications.

2.3. Inverse Model: Machine Learning Model

In the present study, a multilayer perceptron (MLP) was used as the inverse model. A MLP is a fully connected feedforward artificial neural network that produces a set of outputs given a set of inputs. A MLP consists of 3 types of layers: an input layer, hidden layers, and an output layer. In a MLP, data moves forward from the input layer to the output layer. Combined with non-linear activation functions between layers, a MLP can learn complex non-linear relationships between the input and output data [36]. For the research theme at hand, the wavenumbers are used as inputs to predict the elastic stiffness parameters as outputs.

MLPs with one hidden layer have been shown to be universal approximators: In one hidden layer, a MLP can approximate any function, given enough hidden units. However, it is often more efficient to train a network with more than one layer [23]. In the current study, the use of 2 hidden layers turned out to be sufficient to obtain good results. Keras (version: 2.7.0), a Python library for deep learning, was used to implement the MLP [24].

In addition, hyperband optimization was used to determine the number of hidden units per layer [25]. The search space for the optimal number of units was restricted to values between 100 and 5000 units for both layers. Tuning was conducted on 90% of the training data and the other 10% was used for validating the tuned performance. Note that the number of datapoints differs per experiment and therefore the data-set size used in each experiment is specified in the corresponding results section. After finding the optimal set of parameters, the MLP was retrained with this parameter set, now using all training data. Further validation was then conducted using an independent test set.

The performance of the algorithm was assessed by calculating the mean absolute deviation (MAE), the mean absolute percentage deviation (MAPE), and the coefficient of determination (r-squared - R^2). The MAPE measure was used as the cost function and to establish the optimal parameter set during parameter tuning due to its scale-independent nature.

Finally, layer weight regularization was applied to prevent over-fitting. For this, the kernels, biases, and outputs of the layers were regularized. ReLU activation was used on the input layer and hidden layers whereas the Adam optimization method was used with an initial learning rate of 0.001 to train the parameters of the network [26]. The training was done in batches of 256 data points and used a total of 2000 epochs.

Hyperparameters that are not listed in this section were kept to the defaults as provided by Keras. For the calculations, a workstation with NVIDIA® Quadro™ RTX 4000 with 8 GB GDDR6 ram is used.

3. Results and discussion

In this section, the material characterization results using the MLP regression model are reported for a synthetic dataset on the one hand, in order to validate the method, and for an experimental dataset on the other hand to illustrate the method's applicability.

First, numerical dataset simulations are conducted for an orthotropic wooden plate using the forward model SAFE. In the subsequent validation study, the required size of the training data is first analyzed via a parametric search. Then, different percentages of random noise are added to the real wavenumbers in both the training and the test data in order to introduce and mimic suboptimal experimental measurement conditions. The addition of noise on the training and test dataset is crucial to be able to distinguish noise features from other features in order to make the trained models more generalizable.

Following the numerical validation of the inversion method, the proposed stiffness characterization method is then demonstrated on an experimental wavefield dataset of a $[0/90]_{5s}$ G/PA6 laminate.

3.1. Numerical case study: SAFE simulation for a Homogeneous wooden plate

To assess the robustness, accuracy, and computational time of the proposed machine learning method, a numerical case study is conducted on a homogenized orthotropic wooden plate (beech wood) with a thickness of 5 mm and a density of 674 kg/m^3 [27]. Beech wood is an example of a material with a strong anisotropic nature and a low density, which is challenging for

the characterization process. The assumed ground truth values for the elastic stiffness parameters of the material are summarized in Table 1.

Table 1: Beech wood elastic parameters used for the study. Tensor constants are in GPa.

ij	11	12	13	22	23	33	44	55	66
C_{ij}	17.33	3.03	1.69	3.26	0.74	1.64	0.62	1.09	1.52

The full dispersion curve information for this material in different wave propagation directions is calculated by way of the SAFE method and is used to validate the machine learning model. To this end, a frequency range between 10 kHz and 200 kHz with a 10 kHz step size is considered for 0, 45, and 90-degree propagation directions, and the first 5 wave modes of the selected frequency range are selected. This leads to a total of 300 input parameters (20 frequency bins $\times$ 3 propagation directions $\times$ 5 identifiable wave modes) which are subsequently used to estimate 9 stiffness parameters.

In addition, a large training and test dataset is created by way of the SAFE forward method for materials with stiffness values between -40% and +60% of the above mentioned literature values, while the thickness and density are considered fixed. Due to the tendency of classical inversion algorithms to use middle points as initial solutions, non-symmetric parameter bounds are used. These datasets were created by using a random distribution between the search space boundaries of the true stiffness parameters. The distribution of the stiffness parameters are crucial for MLP model to learn the relation between wavenumber and stiffness parameters, and to ac-

curately predict the stiffness parameters through whole boundary range. The histogram of the training and test dataset is represented in Fig. 3.

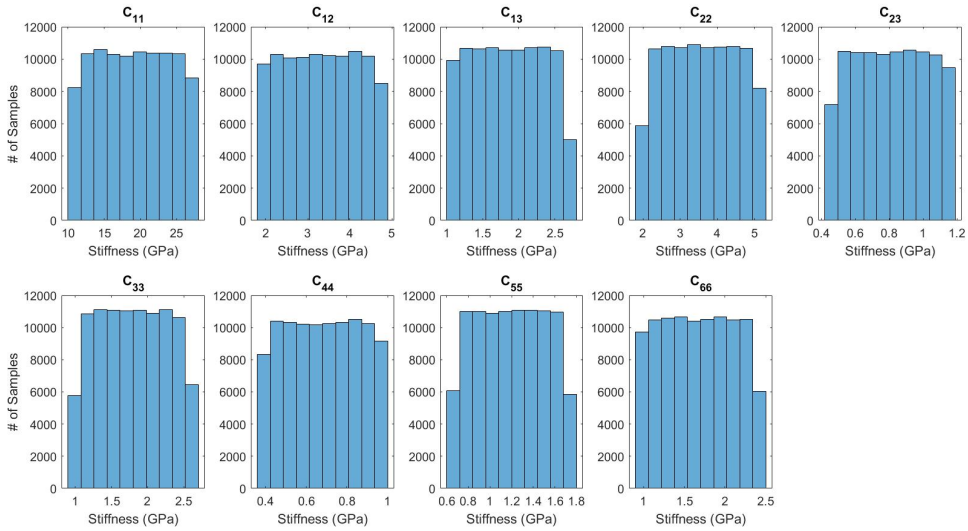

(a)

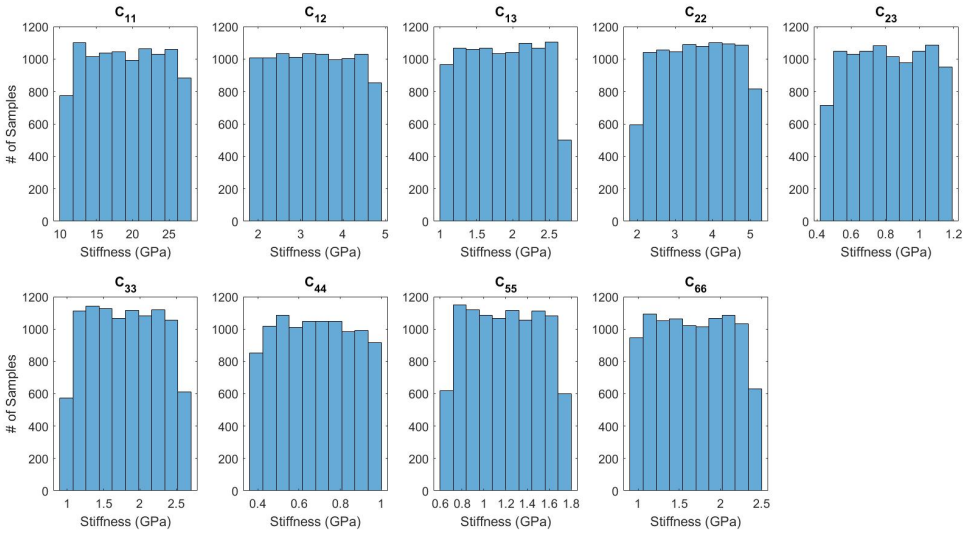

(b)

Figure 3: Histogram of the generated training and test data for the different stiffness parameters a) The distribution of the training data for a collection of 10^5 data points, and b) The distributions of the test data for 10^4 data points.

A search space consisting of 2 layers is created to find the optimum number of units per layer (layer size) of the model using the hyperband algorithm [25] in 'Keras Tuner'. The optimal size of the layers was found to be 3700 for the first hidden layer and 450 for the second layer. The convergence of the MAPE indicator with respect to the training data size is depicted in Fig. 4(a) and shows that a MAPE of about 1.5% can be achieved by using 100 thousand data points, which is an acceptable quantity. As can be seen in the figure, it is possible to further increase the accuracy of the method by simply increasing the size of the dataset, but obviously, the required computational time and power linearly increase with respect to dataset size. In the present study, 100 thousand data points in the dataset was selected, ensuring reasonable accuracy and computational speed. Note that 100 thousand data points correspond to 3.6 data points per stiffness parameter ($3.6^9 \approx 100k$), which shows the extremely sparse nature of the datasets. The full 10^5 point numerical dataset for beech wood as well as the MLP code written in Python can be freely downloaded from [19].

The creation of the dataset (100k) takes 1 hour, and 8 seconds per epoch is required for training. Therefore, in total, only 1.5 hour is required to create the dataset and train the algorithm, while the characterization of the material properties in the inversion step itself is completed instantly. Even though this total duration is already far less than for any known conventional characterization method (typically 3.5 hours including statistics) [10], the true advantage of the MLP regression method is that all calculations can be performed beforehand. After training the MLP, the prediction of a stiffness tensor from a given set of wavenumbers, under the assumption

that all wavenumbers fall within the wavenumber range considered during the training step, takes less than a second. This brings real-time stiffness characterization and model updating within reach.

The convergence of the training and validation data with respect to MAE and loss (MAPE) is plotted in Fig. 4(b) and Fig. 4(c), respectively. The MAE and MAPE plots show a good convergence on both the training and validation dataset, indicating that the MLP is properly trained. A visualization of the predicted versus the real true stiffness parameters for the test datasets is displayed in Fig. 5, confirming a good correlation for most of the stiffness parameters. In fact, only the off-diagonal stiffness parameters (C_{12}, C_{13}, and C_{23})) show increased error levels, which is in line with the sensitivity studies conducted for guided wave modes conducted by Kudela et. al. [28] and for natural frequencies by Gsell et al. [2].

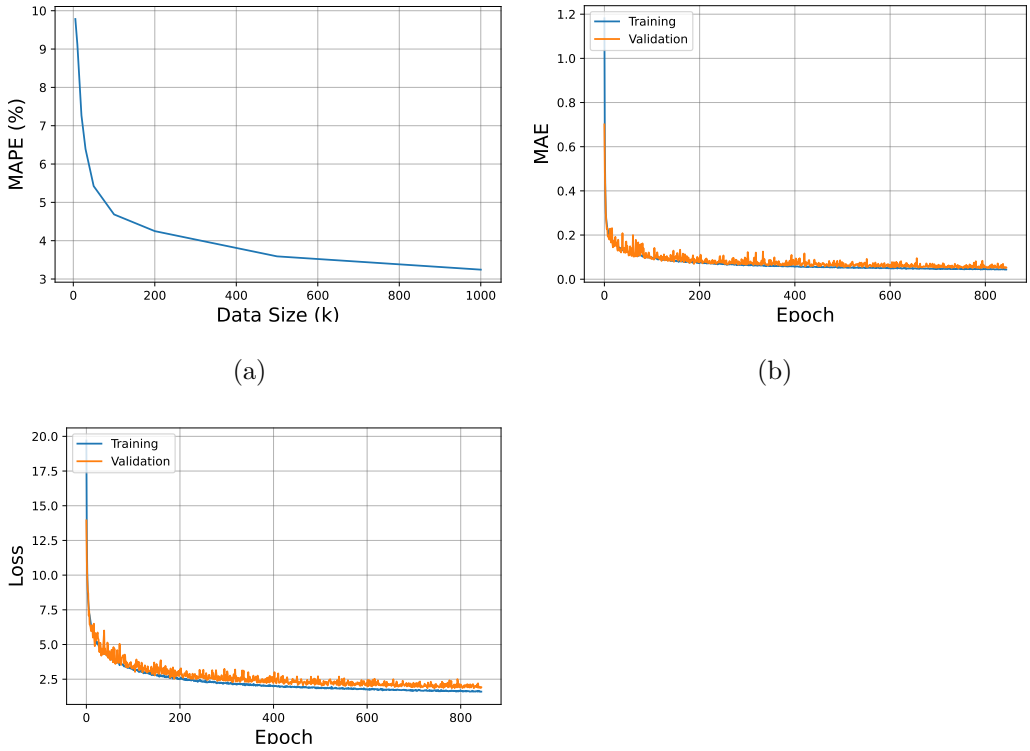

Figure 4: The results of the machine learning algorithm for inverse stiffness characterization for a beech wood plate based on full field dispersion curves. a) The convergence of MAPE of the test data with respect to data size, b) The MAE evolution with respect to epoch number, and c) The loss evolution with respect to epoch number.

For the considered synthetic dataset on the 5mm thick beech wood plate with tensor constants given in Table 1, Table 2 presents an average error level of around 1.5% on the inverted stiffness parameters with respect to the actual stiffness constants in the absence of noise (column 2).

In reality, however, non-zero noise levels might degrade the performance

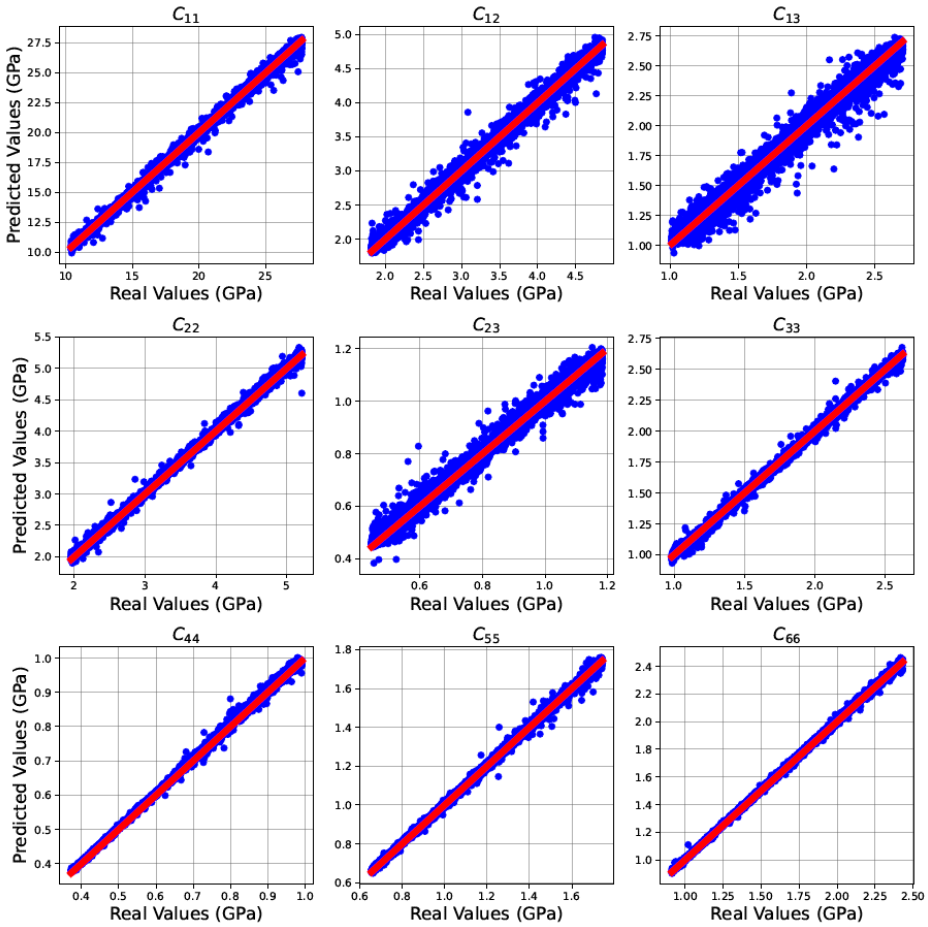

Figure 5: Predicted versus true stiffness parameters for MLP-based inversion of the datasets (blue dots) generated in view of the validation of the method for the case of an orthotropic beech wood plate. As a reference the red line represents the exact match.

of the identification process, leading to higher error rates on the inverted parameters. Therefore, a complementary numerical study is performed in which a random noise level is added to both the training and test data in order to predict the accuracy of the models in the presence of noise. For this study, the noise-affected data is defined as follows:

$$k_{r,noise} = k_r \pm rand(NL)k_r \tag{6}$$

where k_r is the real wavenumber, $k_{r,noise}$ is the real wavenumber perturbed by noise, and $rand(NL)$ is the random noise level with a maximum which is assumed to be 1, 2, 3, 5 and up to 10% in our study.

Again, and for each maximal noise level considered, 'Keras Tuner' is used to optimize the hyperparameters of the model. The average percentage error level of each stiffness component for the beech wood test data considering the different maximal noise levels is shared in Table 2, together with the optimized layer sizes at the respective noise levels. As can be expected, the results show that the accuracy of the predictions decreases when the noise level increase. Still, only a 5.5% average error rate is attained in the presence of 10% noise. Note that, as the accuracy of the extracted wavenumber data depends on the signal-to-noise ratio (SNR) of an experiment, it is possible to train models with various noise ratios and to select one that is close to the experiment.

Table 2: The effect (expressed as the % deviation of the actual C-tensor parameters) of noise (expressed in maximal % digression on the wavenumber data) on the reconstructed C-tensor parameters for a beech wood plate with a density of 674 kg/m^3 and thickness of 5 mm, using a ML approach. The size of the training data (with noise) and test data (with noise) are 100000×300 and 10000×300, respectively. The values in the last two rows denote the layer size in the Keras model after hyperparameter tuning.

Noise (%)	0	1	2	3	5	10
C'_{11}	1.05	1.60	1.79	2.50	2.97	4.23
C'_{12}	2.17	3.12	3.72	4.82	6.55	8.91
C'_{13}	2.69	4.45	5.27	6.48	8.31	11.22
C'_{22}	0.86	1.40	1.76	2.10	2.64	4.16
C'_{23}	2.43	4.02	4.97	6.06	7.36	10.44
C'_{33}	0.83	1.42	1.56	2.01	2.47	3.14
C'_{44}	1.02	1.03	0.80	0.99	1.23	1.39
C'_{55}	0.97	0.89	0.98	1.25	1.41	2.10
C'_{66}	0.60	0.95	0.90	1.09	1.60	2.77
Avg.	1.40	2.10	2.42	3.03	3.84	5.37
Layer I	3700	2700	1400	1900	1850	1450
Layer II	450	4850	1250	850	2550	1950

As shown in Table 2, the error rates of the trained models are on average between 1.5% and 5.5% depending on the considered noise levels. To achieve a higher accuracy, the frequency range and the number of measure-

ment directions can be increased because 1) the sensitivity of the stiffness components strongly correlates with the identification of the cut-off frequencies and the existence of higher-order wave modes, and 2) the orthotropic wave propagation behavior can be more accurately assessed and identified from an increasing number of in-plane directions. However, as this expands the total number of points in the training dataset, the required computational power significantly increases, and high-performance computing (HPC) or cloud-based calculation systems might be needed to manage the ML-based regression.

As a final note based on the numerical validation test considered here, we remark that the above-obtained results and conclusions are in contradiction to the results reported in a recent study [29] in which it is claimed that the dispersion behavior of the two fundamental wave modes (A_0 and S_0) at only two discrete measurement points on the surface is sufficient to invert the full orthotropic stiffness tensor. In that study, an average error of 4.5% is attained based on a dataset created by the semi-analytical finite element model where large boundaries are considered. It should be noted, however, that the study does not allude to a procedure for the elimination of non-physical stiffness parameters in the presence of large inversion boundaries, nor does it provide the details of a mode-tracking algorithm to separate and identify the fundamental modes. Depending on the steps in these procedures, the performance of the algorithm is not guaranteed.

3.2. Numerical case study: COMSOL Simulation for a Homogeneous wooden plate

The studies conducted in the previous section focused on the inversions, in the absence or presence of noise, where both the training and the test datasets are created by means of the SAFE method. However, this above followed approach should be conducted with care to avoid the so-called inverse crime [30, 31]. Inverse crime problems generally occur when the same forward model (predictor) is used to create the synthetic data as well as being adopted during the inversion procedure (estimator). Traditionally, the inverse crime problem is commonly avoided in literature by introducing certain derogations during the inversion procedure, such as adding noise to the predicted data [32]. Applied to our study, the addition of noise in combination with the fact that the dataset is extremely sparse can be considered sufficient to stay away from the inverse crime problem.

Nevertheless, in order to become totally convinced, a supplementary synthetic dataset is created by using COMSOL finite element (FE) simulations to emulate actual experimental measurements. Details of the COMSOL model (See Fig. 6) can be found in literature [10]. The simulations are conducted in the frequency domain, and 300 input parameters (20 frequency bins $\times$ 3 propagation directions $\times$ 5 identifiable wave modes) are extracted by using MPDM and manual post-processing, as explained in Section 2.2 for the experimental data. A random noise level up to 2% is added to the extracted wavenumbers to mimic noise effects comparable with experimental measurements. Subsequently, the MLP model trained in Sec. 3.1 in the presence of 2% noise is used to predict the elastic stiffness parameters. By adopting

this approach 1) the likelihood of an inverse crime is eliminated because the estimator data is created with an independent forward model (COMSOL), different from the model used in the training (SAFE) and 2) Unlike the SAFE model, COMSOL finite element (FE) simulations provide good estimations of the true wave propagation behavior in finite size plates, at least when mesh convergence is guaranteed, because the FE model is able to compute the entire velocity response of the medium in both the spatial and the frequency domain. Additionally, the FE model has the ability to cope with the effect of boundary conditions and edge reflections.

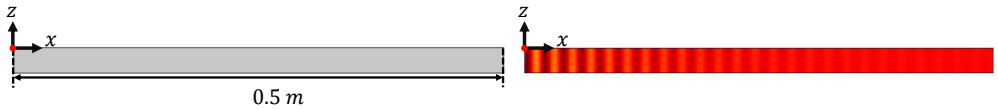

(a) (b)

Figure 6: Model parameters and results of the numerical simulation, a) The geometry and size of the plate in the two-dimensional finite element model, together with the source position, and (b) The displacement field in z direction for beech wood plate with 5 mm thickness (see Table 1 for material properties) at 60 kHz for an in-plane propagation angle $\phi = 0$.

The inverted stiffness parameters derived from the independent wave propagation simulation data are shared in Table 3, and the inversion results are compared with a traditional heuristic algorithm based on Particle Swarm Optimization presented in literature [10]. An average 1.5% error compared to the actual stiffness values as well as to the traditional inversion method is achieved by using the MLP model. The average error on the principal and shear components are found to be around 1.6% and 0.2%, respectively.

The off-diagonal stiffness parameters have relatively higher error rates: on average 2.5%, with the highest error being 5.3% for the C'_{13} component. The obtained error levels are in line with the results obtained in the previous section, indicating that the effect of the inverse crime approach in the above numerical study is not problematic. To further validate the accuracy of the MLP model, the dispersion curves calculated from the inverted stiffness parameters (best match using the SAFE) are superimposed on top of the dispersion data obtained from COMSOL, see Fig. 7.

Table 3: Elasticity values for a 5 mm thick beech wood plate with density 674 kg/m^3 [27], along with the respective inverted homogenized tensor constants obtained by means of the here proposed MLP approach and its comparison with inversion results achieved from a two-stage PSO based inversion algorithm in the presence of 2% noise [10].

	Actual Values	Machine Learning	Traditional Inversion [10]
ij	C'_{ij}	C'_{ij}	C'_{ij}
11	17.33	17.77	17.27($\pm$0.31)
12	3.03	3.10	3.01($\pm$0.42)
13	1.69	1.78	1.68($\pm$0.47)
22	3.26	3.30	3.26($\pm$0.10)
23	0.74	0.74	0.74($\pm$0.16)
33	1.64	1.66	1.64($\pm$0.11)
44	0.62	0.62	0.62($\pm$0.14)
55	1.09	1.09	1.09($\pm$0.01)
66	1.52	1.51	1.52($\pm$0.09)

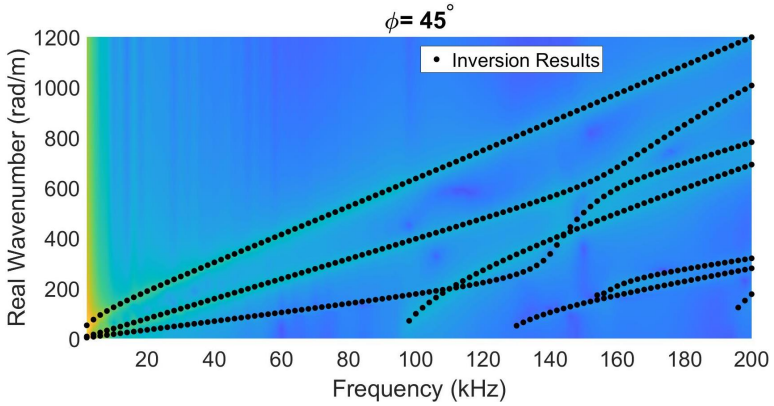

Figure 7: Wavenumber-frequency pairs for in-plane direction $\phi = 45$ corresponding to the MLP optimized stiffness values (black dots) superimposed on the dispersion landscape for a 5 mm thick beech wood plate deduced from the COMSOL Lamb wave propagation data in the same direction.

3.3. Experimental case study: Homogeneous G/PA6 plate

For the experimental case study, Lamb wave propagation data have been acquired on the surface of a cross-ply $[0/90]_{5s}$ G/PA6 laminate with a thickness of 5.5 mm and a density of 1710 kg/m^3. The individual elastic properties of the G/PA6 plies are taken from literature [33], and the homogenized (real) stiffness parameters estimated by accounting for the assumed layer thickness and stacking orientation parameters [34], are listed in column 2 of Table 4. Details on the overall measurement technique and signal acquisition can be found in literature [10]. In this case study, a broadband sweep sine voltage signal with frequencies between 5 kHz to 300 kHz and a total time duration of 16 ms is used. The wavenumber-frequency pairs are automatically extracted by using MPDM [10]. However, to prevent missed data points or to eliminate closely located wavenumbers, the extracted wavenumber-frequency pairs are

further post-processed manually.

The training dataset is again created by using the efficient forward SAFE algorithm for 3 in-plane propagation directions (ϕ = 0, 45, and 90), and 10 frequency points between 60 and 240 kHz with a 20 kHz step size. As for the numerical test case, the first 5 wave modes of the selected frequency range are selected which leads to a total of 150 wavenumber-frequency pairs (10 frequency bins $\times$ 3 propagation directions $\times$ 5 wave modes) used for the training.

The MLP-based inverted stiffness parameters are summarized in the third column of Table 4, and are in reasonable agreement with the homogenized values that were calculated from the individual ply parameters reported in literature. It should be noted, however, that the homogenized literature values are reported for a material with a low-moisture content, and that the actual conditions at the time of the experiment on the composite plate might somewhat deviate with respect to moisture and temperature, which could definitely explain the small discrepancy between literature and inverted stiffness values [33].

In addition and to confirm the acceptability of the inverted stiffness parameters based on the MLP approach, a comparison is again provided between the ML based inversion results and the inversion results obtained by using a traditional heuristic inversion algorithm based on Particle Swarm Optimization [10]. Interestingly, the difference between the results obtained with the traditional inversion method and the proposed MLP-based inversion method is less than 0.5%. Furthermore, in Fig. 8, the computed dispersion curves calculated from the MLP-optimized stiffness parameters (best match

using SAFE) are superposed on the experimentally recorded dispersion landscape. An excellent match is obtained, confirming the high accuracy of the inverted stiffness parameters.

Table 4: Homogenized elasticity values for a 5.5 mm thick multi-layered G/PA6 plate with density 1710 kg/m^3 based on individual ply properties found in literature, and comparison of the here proposed MLP based inversion results with results obtained from a two-stage PSO based inversion algorithm.

	Literature[33]	Machine Learning	Traditional Inversion [10]
ij	C'_{ij}	C'_{ij}	C'_{ij}
11	24.84	21.82	21.87($\pm$0.02)
12	5.10	6.03	6.13($\pm$0.05)
13	5.41	5.35	5.42($\pm$0.01)
22	24.84	23.68	23.53($\pm$0.02)
23	5.41	6.61	6.65($\pm$0.02)
33	12.30	11.88	11.94($\pm$0.02)
44	3.28	2.94	2.94($\pm$0.00)
55	3.28	2.84	2.84($\pm$0.00)
66	3.04	4.27	4.27($\pm$0.01)

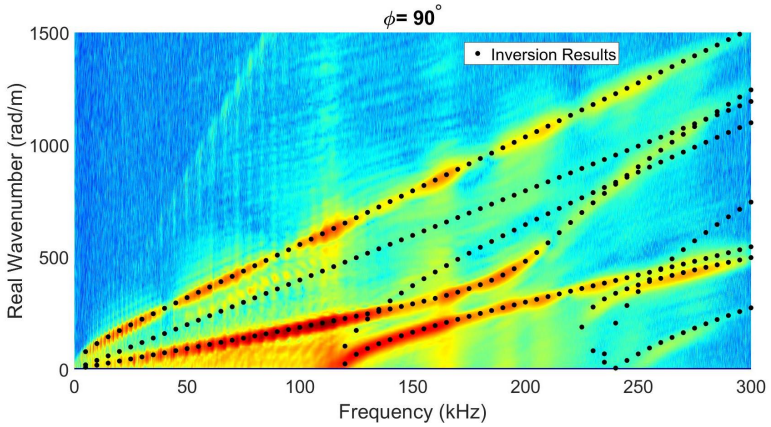

Figure 8: Wavenumber-frequency pairs for in-plane direction $\phi = 90$ corresponding to the MLP optimized stiffness values (black dots) superimposed on the dispersion landscape for a 6 mm thick $[0/90]_{5s}$ cross-ply G/PA6 plate deduced from the experimental Lamb wave propagation data in the same direction.

4. Conclusions

A multilayer perceptron-based inversion scheme has been proposed to identify the elastic stiffness properties of orthotropic plates from the 3D surface velocity response to a broadband vibrational excitation. In the first step, the proposed method extracts the real wavenumber values as a function of frequency from the experimental wave propagation datasets at different in-plane directions using the matrix pencil decomposition method (MPDM). Alongside, for the inversion, the dispersion behavior for a large number of materials with a range of orthotropic elastic stiffness parameters is simulated by a fast semi-analytical finite element (SAFE) method. The resulting simulation database thus consists of a large set of directional wavenumber-frequency values which are used to train a multilayer perceptron algorithm in view of identifying the targeted orthotropic elastic stiffness parameters.

The proposed inversion method is first validated using a synthetic dataset created by SAFE, representative for a wooden plate, showing excellent performance with an average relative error of 1.5% in the absence of noise, and increasing up to 5.5% in the presence of 10% noise. Next, the same procedure is applied on a numerical dataset created by an independent forward finite element (COMSOL) model in the presence of 2% noise, resulting in a similar 1.5% average error, and thereby verifying the negligible effect of an inverse crime approach in the applied procedure. Finally, further validation of the MLP method is obtained on experimentally measured 3D Infrared Scanning Laser Doppler Vibrometry data for a 5.5. mm thick cross-ply glass fiber reinforced polyamide plate. The inverted stiffness parameters are compared with the results of a traditional inversion method, showing less than 0.5% average difference. In addition, a good agreement with the homogenized stiffness values reported in literature is found.

The main benefit of the proposed multilayer perceptron-based inversion method is that, following a training stage which can be programmed in advance, the method yields accurate estimates of the elastic parameters of orthotropic plates within a second, which makes it particularly useful for real-time structural health monitoring and online model calibration and updating.

References

[1] J. Segers, S. Hedayatrasa, G. Poelman, W. Van Paepegem, M. Kersemans, Backside delamination detection in composites through local de-

fect resonance induced nonlinear source behavior, Journal of Sound and Vibration (2020) 115360.

[2] D. Gsell, G. Feltrin, S. Schubert, R. Steiger, M. Motavalli, Cross-laminated timber plates: Evaluation and verification of homogenized elastic properties, Journal of structural engineering 133 (1) (2007) 132–138.

[3] R. Longo, D. Laux, S. Pagano, T. Delaunay, E. Le Clézio, O. Arnould, Elastic characterization of wood by resonant ultrasound spectroscopy (rus): a comprehensive study, Wood science and technology 52 (2) (2018) 383–402.

[4] B. V. Damme, S. Schoenwald, A. Zemp, Modeling the bending vibration of cross-laminated timber beams, European journal of wood and wood products 75 (6) (2017) 985–994.

[5] A. Santoni, P. Bonfiglio, F. Mollica, P. Fausti, F. Pompoli, V. Mazzanti, Vibro-acoustic optimisation of wood plastic composite systems, Construction and Building Materials 174 (2018) 730–740.

[6] J. Vishnuvardhan, C. Krishnamurthy, K. Balasubramaniam, Determination of material symmetries from ultrasonic velocity measurements: a genetic algorithm based blind inversion method, Composites science and technology 68 (3-4) (2008) 862–871.

[7] A. Martens, M. Kersemans, J. Daemen, E. Verboven, W. Van Paepegem, S. Delrue, K. Van Den Abeele, Characterization of

the orthotropic viscoelastic tensor of composites using the ultrasonic polar scan, Composite Structures 230 (2019) 111499. doi:https://doi.org/10.1016/j.compstruct.2019.111499.
URL https://www.sciencedirect.com/science/article/pii/S0263822319311274

[8] M. Sale, P. Rizzo, A. Marzani, Semi-analytical formulation for the guided waves-based reconstruction of elastic moduli, Mechanical Systems and Signal Processing 25 (6) (2011) 2241–2256.

[9] P. Kudela, M. Radzienski, P. Fiborek, T. Wandowski, Elastic constants identification of fibre-reinforced composites by using guided wave dispersion curves and genetic algorithm for improved simulations, Composite Structures 272 (2021) 114178.

[10] A. H. Orta, M. Kersemans, K. Van Den Abeele, On the identification of orthotropic elastic stiffness using 3d guided wavefield data, Sensors 22 (14) (2022). doi:10.3390/s22145314.
URL https://www.mdpi.com/1424-8220/22/14/5314

[11] L. Araque, L. Wang, A. Mal, C. Schaal, Advanced fuzzy arithmetic for material characterization of composites using guided ultrasonic waves, Mechanical Systems and Signal Processing 171 (2022) 108856. doi:https://doi.org/10.1016/j.ymssp.2022.108856.
URL https://www.sciencedirect.com/science/article/pii/S088832702200053X

[12] D. Bobylev, T. Choudhury, J. O. Miettinen, R. Viitala, E. Kurvinen,

J. Sopanen, Simulation-based transfer learning for support stiffness identification, IEEE Access 9 (2021) 120652–120664.

[13] H. Liu, Z. Zhang, H. Jia, Q. Li, Y. Liu, J. Leng, A novel method to predict the stiffness evolution of in-service wind turbine blades based on deep learning models, Composite structures 252 (2020) 112702.

[14] A. Wei, J. Xiong, W. Yang, F. Guo, Deep learning-assisted elastic isotropy identification for architected materials, Extreme Mechanics Letters 43 (2021) 101173.

[15] M. Rautela, S. Gopalakrishnan, K. Gopalakrishnan, Y. Deng, Ultrasonic guided waves based identification of elastic properties using 1d-convolutional neural networks, in: 2020 IEEE International Conference on Prognostics and Health Management (ICPHM), 2020, pp. 1–7. doi:10.1109/ICPHM49022.2020.9187057.

[16] K. Gopalakrishnan, M. Rautela, Y. Deng, Deep learning based identification of elastic properties using ultrasonic guided waves, in: P. Rizzo, A. Milazzo (Eds.), European Workshop on Structural Health Monitoring, Springer International Publishing, Cham, 2021, pp. 77–90.

[17] M. Rautela, A. Huber, J. Senthilnath, S. Gopalakrishnan, Inverse characterization of composites using guided waves and convolutional neural networks with dual-branch feature fusion, Mechanics of Advanced Materials and Structures 29 (27) (2021) 1–17. arXiv:https://doi.org/10.1080/15376494.2021.1982090, doi:10.1080/15376494.

2021.1982090.
URL https://doi.org/10.1080/15376494.2021.1982090

[18] T. Cohen, M. Welling, Group equivariant convolutional networks, in: International conference on machine learning, PMLR, 2016, pp. 2990–2999.

[19] A. H. Orta, J. De Boer, M. Kersemans, C. Vens, K. Van Den Abeele, Ml-mac, https://github.com/adilorta/ML-MaC.git (2022 (accessed 20-December-2022)).

[20] I. Bartoli, A. Marzani, F. L. di Scalea, E. Viola, Modeling wave propagation in damped waveguides of arbitrary cross-section, Journal of Sound and Vibration 295 (3-5) (2006) 685–707.

[21] A. H. Orta, M. Kersemans, K. Van Den Abeele, The dispersion box, https://github.com/adilorta/The-Dispersion-Box.git (2022 (accessed 12-January-2022)).

[22] A. H. Orta, M. Kersemans, K. Van Den Abeele, A comparative study for calculating dispersion curves in viscoelastic multi-layered plates, Composite Structures 294 (2022) 115779. doi:https://doi.org/10.1016/j.compstruct.2022.115779.
URL https://www.sciencedirect.com/science/article/pii/S0263822322005530

[23] R. Reed, R. J. MarksII, Neural smithing: supervised learning in feedforward artificial neural networks, Mit Press, 1999.

[24] F. Chollet, keras, https://github.com/fchollet/keras (2015).

[25] L. Li, K. Jamieson, G. DeSalvo, A. Rostamizadeh, A. Talwalkar, Hyperband: A novel bandit-based approach to hyperparameter optimization, The Journal of Machine Learning Research 18 (1) (2017) 6765–6816.

[26] D. P. Kingma, J. Ba, Adam: A method for stochastic optimization, arXiv preprint arXiv:1412.6980 (2014).

[27] V. Bucur, F. Rocaboy, Surface wave propagation in wood: prospective method for the determination of wood off-diagonal terms of stiffness matrix, Ultrasonics 26 (6) (1988) 344–347. doi:https://doi.org/10.1016/0041-624X(88)90033-9.
URL https://www.sciencedirect.com/science/article/pii/0041624X88900339

[28] P. Kudela, M. Radzienski, P. Fiborek, T. Wandowski, Elastic constants identification of woven fabric reinforced composites by using guided wave dispersion curves and genetic algorithm, Composite Structures 249 (2020) 112569.

[29] S. Wang, Z. tao Luo, J. Jing, Z. hao Su, X. kai Wu, Z. hua Ni, H. Zhang, Real-time determination of elastic constants of composites via ultrasonic guided waves and deep learning, Measurement 200 (2022) 111680. doi:https://doi.org/10.1016/j.measurement.2022.111680.
URL https://www.sciencedirect.com/science/article/pii/S0263224122008880

[30] D. L. Colton, R. Kress, R. Kress, Inverse acoustic and electromagnetic scattering theory, Vol. 93, Springer, 1998.

[31] A. Wirgin, The inverse crime (2004). doi:10.48550/ARXIV.MATH-PH/0401050.
URL https://arxiv.org/abs/math-ph/0401050

[32] D. Potyagaylo, W. H. Schulze, O. Doessel, A new method for choosing the regularization parameter in the transmembrane potential based inverse problem of ecg, in: 2012 Computing in Cardiology, IEEE, 2012, pp. 29–32.

[33] D. P. Raghavalu Thirumalai, T. Løgstrup Andersen, A. Lystrup, Influence of moisture absorption on properties of fiber reinforced polyamide 6 composites, Proceedings of the 26th Annual Technical Conference of the American Society for Composites (2011).

[34] J. N. Reddy, Mechanics of laminated composite plates and shells: theory and analysis, CRC press, 2003.

[35] Y. Li, J. Zhu, M. Duperron, P. O'Brien, R. Schüler, S. Aasmul, M. Melis, M. Kersemans, R. Baets, Six-beam homodyne laser Doppler vibrometry based on silicon photonics technology, Optics Express (26) 2018, 3638

[36] I. Goodfellow, Y. Bengio, A. Courville, Deep Learning, MIT Press, 2016.

[37] S. Sabeti, W. H. Schulze, J.B. Harley, Spatio-temporal undersampling: Recovering ultrasonic guided wavefields from incomplete data with compressive sensing, Mechanical Systems and Signal Processing (140) 2020, 106694.